Geophysical Journal International

Geophys. J. Int. (2014) **198,** 1805–1817 doi: 10.1093/gji/ggu239

GJI Geomagnetism, rock magnetism and palaeomagnetism

Relevant magnetic and soil parameters as potential indicators of soil conservation status of Mediterranean agroecosystems

Laura Quijano,[1] Marcos A.E. Chaparro,[2] Débora C. Marié,[2] Leticia Gaspar[3] and Ana Navas[1]

[1] *Estación Experimental de Aula Dei, Consejo Superior de Investigaciones Científicas (EEAD-CSIC), P.O. Box* 13034, *E-*50080 *Zaragoza, Spain. E-mail: lquijano@eead.csic.es*

[2] *CONICET and CIFICEN Universidad Nacional del Centro de la Provincia de Buenos Aires, Pinto* 399, 7000 *Tandil, Argentina*

[3] *Cranfield Water Sciences Institute, University of Cranfield, Cranfield, Bedfordshire MK*43 0*AL, United Kingdom*

Accepted 2014 June 20. Received 2014 June 18; in original form 2013 December 10

SUMMARY

The main sources of magnetic minerals in soils unaffected by anthropogenic pollution are iron oxides and hydroxides derived from parent materials through soil formation processes. Soil magnetic minerals can be used as indicators of environmental factors including soil forming processes, degree of pedogenesis, weathering processes and biological activities. In this study measurements of magnetic susceptibility are used to detect the presence and the concentration of soil magnetic minerals in topsoil and bulk samples in a small cultivated field, which forms a hydrological unit that can be considered to be representative of the rainfed agroecosystems of Mediterranean mountain environments.

Additional magnetic studies such as isothermal remanent magnetization (IRM), anhysteretic remanent magnetization (ARM) and thermomagnetic measurements are used to identify and characterize the magnetic mineralogy of soil minerals. The objectives were to analyse the spatial variability of the magnetic parameters to assess whether topographic factors, soil redistribution processes, and soil properties such as soil texture, organic matter and carbonate contents analysed in this study, are related to the spatial distribution pattern of magnetic properties. The medians of mass specific magnetic susceptibility at low frequency (χ_{lf}) were 36.0 and 31.1 $\times$ 10^{-8} m^3 kg^{-1} in bulk and topsoil samples respectively. High correlation coefficients were found between the χ_{lf} in topsoil and bulk core samples ($r = 0.951, p < 0.01$). In addition, volumetric magnetic susceptibility was measured *in situ* in the field (κ_{is}) and values varied from 13.3 to 64.0 $\times$ 10^{-5} SI. High correlation coefficients were found between χ_{lf} in topsoil measured in the laboratory and volumetric magnetic susceptibility field measurements ($r = 0.894$, $p < 0.01$). The results obtained from magnetic studies such as IRM, ARM and thermomagnetic measurements show the presence of magnetite, which is the predominant magnetic carrier, and hematite. The predominance of superparamagnetic minerals in upper soil layers suggests enrichment in pedogenic minerals. The finer soil particles, the organic matter content and the magnetic susceptibility values are statistically correlated and their spatial variability is related to similar physical processes. Runoff redistributes soil components including magnetic minerals and exports fine particles out the field. This research contributed to further knowledge on the application of soil magnetic properties to derive useful information on soil processes in Mediterranean cultivated soils.

Key words: Spatial analysis; Environmental magnetism; Magnetic mineralogy and petrology; Remagnetization; Geomorphology; Europe.

1 INTRODUCTION

Magnetic minerals such as iron oxides and hydroxides are very sensitive to physico-chemical conditions in sedimentary environments (Evans & Heller 2003). The properties of soil magnetic minerals and its related magnetic parameters are applied in a variety of studies, associated with the interpretation of environmental processes (Liu *et al.* 2012). Soil magnetic minerals are used as indicators for anthropogenic pollution monitoring (Chaparro *et al.* 2006; Blundell *et al.* 2009) pedogenic processes related to the formation of

magnetic minerals (Bidegain *et al.* 2009; Liu *et al.* 2010; Torrent *et al.* 2010a), soil degradation (Royall 2001; Sadiki *et al.* 2009) and soil redistribution processes by agricultural practices (Jordanova *et al.* 2011, 2012).

Soil magnetic properties depend on the concentration and characteristics (shape, size and composition) of magnetic minerals (Mullins 1977). The classification of magnetic components in natural samples in terms of mineralogy, domain state, and concentration, is important for assessing the nature and origin of the components (Peters & Dekkers 2003).

A rapid and non-destructive technique to assess magnetic iron–mineral contents is the measure of the mass specific magnetic susceptibility (Thompson & Oldfield 1986; Walden *et al.* 1999). *In situ* measurements of volumetric magnetic susceptibility using field probes have also proved to be useful tools for mapping and screening magnetic susceptibility of topsoils in areas with low pollution impact (Kapicka *et al.* 2001; Chaparro *et al.* 2007). Mass specific magnetic susceptibility (χ) is a magnetic mineral concentration-dependent parameter. According to its value (order and sign), materials are classified as diamagnetic with negative and low χ values ($\sim -6 \times 10^{-9}$ m^3 kg^{-1}), paramagnetic with positive and higher values than diamagnetic ones ($\sim 10^{-6}$ m^3 kg^{-1}), antiferromagnetic (~ 6–7×10^{-7} m^3 kg^{-1}) and ferrimagnetic materials with positive and the highest mass specific magnetic susceptibility values (~ 0.5–5.6×10^{-3} m^3 kg^{-1}, in detail in Maher *et al.* 1999).

Measurements of mass specific magnetic susceptibility at low (0.47 kHz; χ_{lf}) and high (4.7 kHz; χ_{hf}) frequency allow to determine absolute mass specific dual frequency-dependent susceptibility (χ_{fd}), defined as the difference between the measure at low and high frequencies ($\chi_{fd} = \chi_{lf} - \chi_{hf}$). Alternatively, this parameter is commonly expressed as a percentage, that is the percentage frequency-dependent susceptibility ($\chi_{fd}\%$) using the following equation:

$$\chi_{fd}\% = [(\chi_{lf} - \chi_{hf})/\chi_{lf}) \times 100].$$

The χ_{fd} is proportional to the concentration of ultrafine (<0.03 μm; superparamagnetic grains, SP) ferrimagnetic particles and if SP grains dominate the assemblage, χ_{fd} can be used semi-quantitatively to estimate their concentration (Dearing *et al.* 1997). The values of $\chi_{fd}\%$ are inversely related to the grain size distribution of these superparamagnetic particles and according to their values it is possible to interpret the $\chi_{fd}\%$ data semi-quantitatively as dominance or admixtures of SP and coarser grains (Dearing *et al.* 1996; Worm 1998).

The anhysteretic remanent magnetization (ARM) and isothermal remanent magnetization (IRM) are artificial remanences obtained in the laboratory and their derived magnetic parameters, that is: SIRM, *S*-ratio, χ_{ARM}, that inform about concentration and domain state (grain size) of the magnetic minerals. Magnetic susceptibility enhancement in upper soil layers and the preferential concentration of magnetic minerals in the clay fraction were reported by Le Borgne (1955). Magnetic enhancement is related to the formation of fine-grained strongly magnetic minerals (pedogenic magnetite/maghemite) in soils (Lu *et al.* 2012), the preferential accumulation of magnetic minerals that resist weathering (Singer *et al.* 1996) and/or anthropogenic processes such as the deposition of combustion subproducts of fossil fuels (Flanders 1999; Chaparro *et al.* 2010; Zhang *et al.* 2012).

Soil iron components are good markers of soil development. Thereof measurements of magnetic properties could be useful to an approximation of soil-forming environment and the intensity of pedogenesis (Maher 1998). In addition, the spatial variation of magnetic soil properties along a slope can be used as an indicator of soil redistribution processes and soil development. Slope positions affect the spatial distribution of soil properties, especially in small, low-relief areas (Qin *et al.* 2012).

Mediterranean agroecosystems are sensitive areas to soil degradation due to severe climate conditions and anthropogenic pressure. Soil magnetic properties combined with physiographic and edaphic parameters offer potential tools for the interpretation of soil processes in agroecosystems, however to date such studies are scarce for the Mediterranean region. In this study, magnetic parameters such as mass specific and volumetric magnetic susceptibility and different artificial remanent magnetizations were measured from soils in a cultivated hydrological unit selected as being representative of rainfed agroecosystems in Mediterranean mountain environments. The objectives were: (i) to establish the spatial pattern of mass specific and volumetric magnetic susceptibility changes in the cultivated field and to assess if soil morphological attributes such as elevation and slope are related to magnetic susceptibility, (ii) to study the relationship between particle-size distribution and the values of magnetic susceptibility, (iii) to infer the relationships between magnetic susceptibility, topography and soil redistribution processes and (iv) to compare the measurements of magnetic susceptibility with the MS2D field probe and the laboratory data with the MS2B sensor. Furthermore, analyses of soil magnetic properties, that is: ARM, IRM, *S*-ratio are proposed in order to gain a better understanding of the soil magnetic mineralogy and infer its origin and contribution to magnetic enhancement. A new experimental method that applies IRM acquisition and demagnetizing alternating field (Chaparro & Sinito 2004; Chaparro *el al*. 2005) will be used to discriminate magnetic phases. In this method, parameters and curves are related to the magnetic mineralogy of each phase. Thermomagnetic measurements will be also applied to identify the magnetic mineralogy. This research will contribute to gain knowledge on the application of soil magnetic properties to infer its relationships with soil processes in cultivated Mediterranean soils.

2 MATERIALS AND METHODS

The study site is a small cultivated field of 3846 m^2 located in the central part of the Ebro Basin (northeast Spain) 42°25′38.52′N; 1°13′14.04′W (Fig. 1a). The study area is a hydrological unit and was defined on the basis of a detailed digital elevation model (DEM) together with field observations. The DEM of the study area was created using a total topographic station to obtain elevation data on a regular 5 × 5 m grid. A gully system drains the field and exports runoff and eroded soil particles to the main ephemeral stream (Figs 1b and c).

The soils in the study area were classified as Calcisols developed on Tertiary clays and sandstones. The soils have low organic matter content (0.4–1.6 per cent), high carbonate contents (31–49 per cent) and the soil textures are silt loam (67 per cent), silty clay loam (17 per cent), sandy loam (8 per cent), loam (5 per cent) and clay (3 per cent). Sandy loam textures were only found at downslope positions. The field has been cultivated for more than 150 yr and consequently the soil is thoroughly mixed in the plough layer (25–30 cm). *In situ* field observations revealed that soil redistribution from tillage occurs although to a lesser extent than water erosion, which is triggered by the gully system.

The average altitude of the study area is 632 m a.s.l. The study field can be divided into three main physiographic parts. The upper

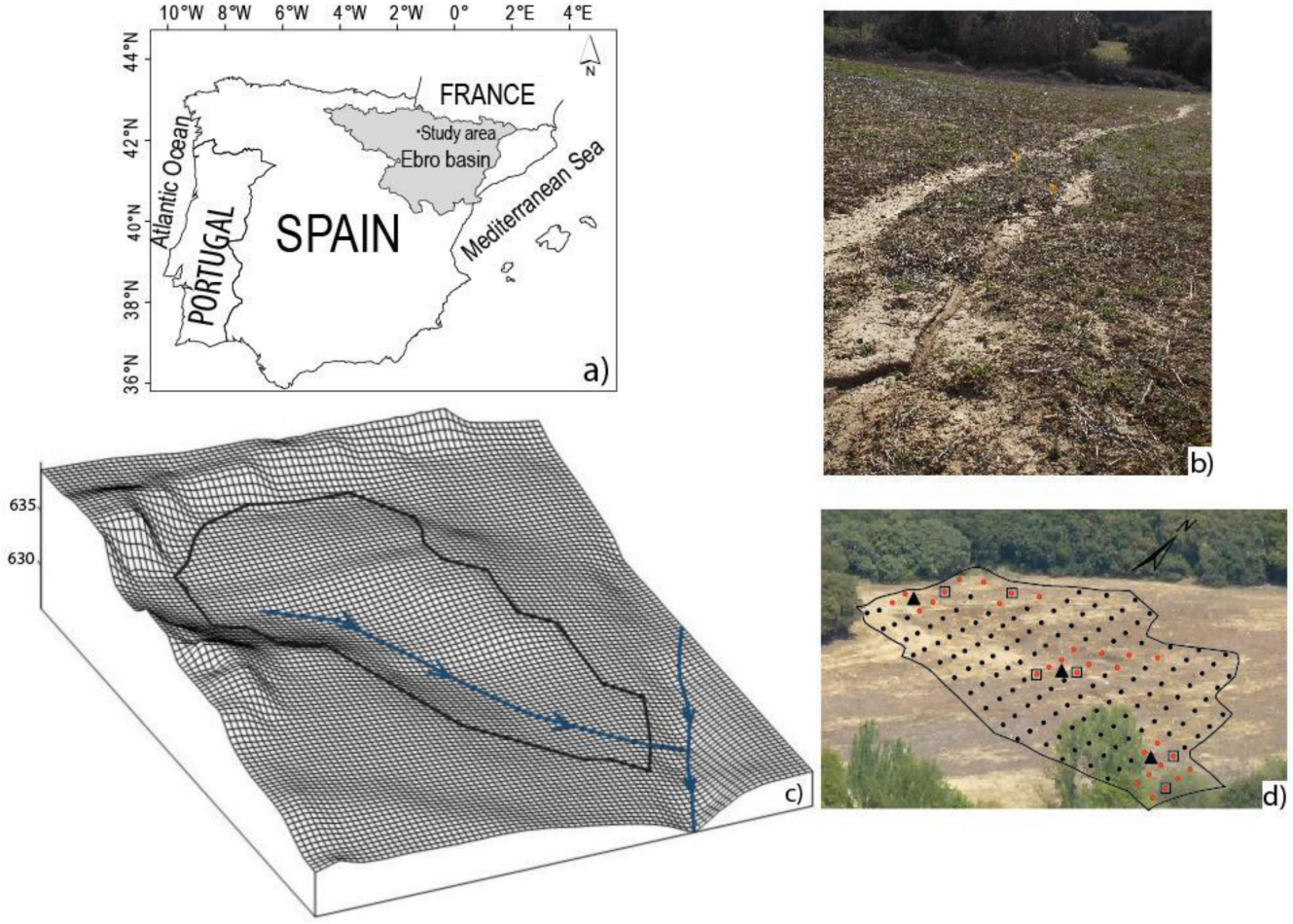

Figure 1. (a) Location of the study area in the central part of the pre-Pyrenees (NE Spain); (b) gully system at middle slope position; (c) 2-D view of the digital elevation model of the study area; (d) view of the study area and soil sampling sites ($n = 154$). Thirty soil sampling points were selected for magnetic studies, they are marked with red circles; black triangles indicate the three locations where soil depth profiles were collected. Soil samples analysed by thermomagnetic curves are marked with black squares.

part is a relatively flat interrill area, not incised by the gully that is well developed in the middle and bottom parts of the field. The climate is continental Mediterranean, characterized by dry summers and heavy rainfall events mainly occurring in spring (April and May) and autumn (September and October), otherwise precipitation is generally scarce. Mean annual rainfall is around 500 mm and mean annual temperature is 13.4 °C.

A total of 154 sampling sites were established on a 5 × 5 m grid to collect topsoil and bulk core samples (Fig. 1d). The topsoil samples ($n = 154$) were collected with a 4 cm diameter manual core drill at a depth of 5 cm. The bulk core profile samples ($n = 154$) were collected using a 7 cm diameter automatic core drill. The sampling depth corresponded with the thickness of the plough layer (30 cm) and if the site was considered to be a deposition site, by field observation, the sampling depth was increased to 50 cm. In addition, three soil depth profiles were collected at upper, middle and bottom slope positions respectively, to a depth of 40 cm (Fig. 1d). A 7-cm-diameter manual core drill was used for soil sampling at 5 cm intervals.

Soil samples were air-dried and passed through a 2-mm sieve to remove gravel fractions and then packed, weighed, labelled and stored at 4 °C prior to the analyses.

In the laboratory, mass specific magnetic susceptibility was measured in 10 ml topsoil and bulk soil samples at both low (0.47 kHz; χ_{lf}) and high (4.7 kHz; χ_{hf}) frequencies using a Bartington Instruments dual-frequency MS2B sensor that operates with an alternating current producing an alternating magnetic field at 80 A m^{-1} (Bartington Instruments Ltd. 2000). Mass specific magnetic susceptibility at low and high frequency measurements was expressed as 10^{-8} m^3 kg^{-1}. The results presented in this study are the mean value of three measurements.

Field measurements of surface volumetric magnetic susceptibility (κ_{is}) were carried out using a MS2 magnetic susceptibility meter and MS2D probe handle. κ_{is} was measured on the same sampled 5 × 5 m grid and the MS2D loop was placed into contact with the soil surface next to the sampling point. Volumetric magnetic susceptibility is dimensionless and it was reported in 10^{-5} SI.

MS2D sensor integrates the magnetic signal within an effective range of its coil. In general, the contribution comes from an area of about 270 cm^2 and the top 6–10 cm of the land surface. According to Dearing (1999) the sensitivity of the MS2D loop is 90 per cent and 10 per cent at 2 and 60 mm from the contact surface, respectively. Moreover, Lecoanet *et al.* (1999) carried out a study proving that 95 per cent of the magnetic susceptibility recorded comes from the uppermost 8 cm (depth penetration) of the measuring surface. The results presented are the mean value of three measurements made at each point in the field. The surface of the MS2D loop sensor cannot be completely in contact with the soil surface thus the sensor is

calibrated according to the surface roughness. On rough soil surface the sensor is calibrated to read 0.5 of the volumetric magnetic susceptibility value and on smooth surfaces as in the study field it is calibrated to read 0.75 of the volumetric magnetic susceptibility value so the mean value of κ_{is} was corrected according to the equipment recommendations (Bartington Instruments Ltd. 2000).

Particle-size analysis was carried out on bulk soil samples ($n = 154$) with a Beckman Coulter LS 13 320 laser diffraction particle size analyser using the Fraunhofer model based on Fraunhofer theory of light scattering combined with Beckman Coulter's patented Polarization Intensity Differential Scattering (PIDS) technology. These two readings are combined to provide a continuous particle size range of 0.017–2000 μm.

According to Murray (2002), the Fraunhofer optical model was preferred to carry out the particle size analyses in carbonate rich soils.

Before textural analysis the organic matter was eliminated by pretreating the soil samples with H_2O_2 (10 per cent) heated to 80 °C. The soil samples were then air dried and chemically disaggregated with 2 cc of sodium hexametaphosphate (40 per cent) and stirred for 2 hr after which they were dispersed with ultrasound for a few minutes.

Soil texture data are compositional and require special considerations before the application of standard multivariate analysis (Loosvelt *et al.* 2013). For this purpose clay, silt and sand contents were transformed based on the additive log-ratio methodology proposed by Aitchison (1982, 1986). Statistical analyses from untransformed and transformed data have been compared to select the most significant correlations.

Organic matter and carbonate content were analysed in bulk soil samples on a 10 × 10 m grid ($n = 40$). Organic matter content (OM) was determined by the wet oxidation method using a titrimeter with selective electrode and carbonate content was measured using a pressure calcimeter (CSIC 1976).

An analysis of the spatial distribution of magnetic susceptibility and the primary topographic attributes derived directly from the DEM (Wilson & Gallant 2000) was made using Arc GIS 10.0 software. The Ordinary Kriging method was used to interpolate the magnetic susceptibility data into a continuous map.

The data were analysed by SPSS version 19 for Windows. ANOVA and Kruskal–Wallis tests were performed to analyse the difference between the means and medians of different groups.

Factor analysis was used to reduce and simplify the representation of the relationships between a set of interrelated variables. The number of factors was determined using the eigenvalue-one criterion, which determines that factors with eigenvalues greater than 1 are to be extracted. The applicability of the factor analysis in the data sets used in this study was verified by applying Bartlett's sphericity and Kaiser–Meyer–Olkin (KMO) tests.

Thirty soil samples were selected from bulk samples at three different slope positions (marked with red circles in Fig. 1d). Ten samples for each part of the slope (upslope, middle and bottom slope) were chosen in order to account for soil processes related with the topographical position along the slope that might influence soil magnetic properties. The selected 30 soil samples were subsampled for detailed magnetic studies using plastic containers (2.3 cm^3). Subsequently the samples were fixed using sodium silicate to prevent unwanted movements in studies of remanence magnetization. From the magnetic point of view, non-destructive magnetic susceptibility measurements were carried out followed by destructive measurements, that is anhysteretic remanent magnetization and isothermal remanent magnetization acquisition.

ARM was acquired using a partial ARM (pARM) device attached to a shielded demagnetizer Molspin Ltd., superimposing a dc bias field of 90 μT to an alternating magnetic field (AF) of 100 mT, during its decay [100; 2.5 mT] and an AF decay rate of 17 μT per cycle. The remanent magnetization was measured by a spinner fluxgate magnetometer Minispin, Molspin Ltd. Anhysteretic susceptibility (κ_{ARM}) was estimated using linear regression for ARM acquired at different DC bias fields (7.96, 47.75 and 71.58 A m^{-1}). Related parameters, such as, King's plot (κ_{ARM} versus κ, King *et al.* 1982) and the κ_{ARM}/κ-ratio were also calculated.

IRM was acquired using a pulse magnetizer model IM-10–30 ASC Scientific. Each sample was magnetized by exposing it to growing stepwise dc fields, 27 forward steps from 4.3 to 2470 mT. The remanent magnetization after each step was measured using the above-mentioned Minispin magnetometer. In these measurements, IRM acquisition curves and SIRM were found using forward dc fields. Remanent coercivity (H_{CR}, the backfield required to remove the SIRM, or IRM = 0) and S-ratio (= $-IRM_{-300}$/SIRM, where IRM_{-300} is the acquired IRM at a backfield of 300 mT) were also calculated from IRM measurement, using a series of backfield demagnetization measurements allow the SIRM acquisition.

Additional measurements using a new experimental method (Chaparro & Sinito 2004) were carried out in order to discriminate magnetic phases. The method is based on the responses of different assemblages of magnetic materials when they are subjected to a pulse-magnetizing field and a demagnetizing alternating field and it separates the bulk backfield IRM curve into two individual magnetic phases experimentally. As indicated by Chaparro *et al.* (2005), the method is only carried out for backfield IRM measurements. First, backfield measurements without AF demagnetization are conducted [backIRM(#i), i indicates the backfield magnetization step]. Once the entire process has finished the sample is demagnetized and subsequently subjected to a dc field to acquire its corresponding SIRM again. Secondly, the residual backfield measurements are carried out, that is after each backfield magnetization step; an AF demagnetization at n mT peak value is performed. In this way a residual remanent magnetization [backIRMn(#i)] is measured at each stage of the method.

In this study separation was achieved using a high peak AF value ($n = 102.5$ mT) as the filter. This AF value is chosen according to the markedly different response of soft and hard magnetic materials. From both measurements, the backIRM(#i) and backIRM102.5(#i), two magnetic phases (Phases 1 and 2), obtained by subtraction can be drawn,

$$\text{Phase2}(\#i) = \text{backIRM102.5}(\#i)$$
$$\text{Phase1}(\#i) = \text{backIRM}(\#i) - \text{backIRM102.5}(\#i).$$

Based on this discrimination, it is possible to calculate the SIRM for each phase and its corresponding magnetic contribution (per cent) to the total SIRM, as well as, the H_{CR} and S-ratio for each phase.

Thermomagnetic measurements were carried out on six soil samples (0.4–0.5 g) using a home-made horizontal magnetic translation balance (Escalante & Böhnel 2011) built in the Laboratory of Palaeomagnetism (Centro de Geociencias, UNAM, University of Mexico). This instrument measures the temperature dependence of high-field magnetization; basically it measures the force on specimens subjected to a magnetic gradient (Collinson 1983), which is compensated by an electronic feedback system to hold the specimen in a fixed position. The non-uniform field was produced by an electromagnet with special shape of pole pieces, which was controlled during the experiment with a power supply at constant current. At

Table 1. Basic statistics of mass specific and volumetric magnetic susceptibility and soil texture.

$n = 154$	χ_{lf} bulk 10^{-8} m^{3}kg^{-1}	χ_{hf} bulk 10^{-8} m^{3}kg^{-1}	χ_{lf} topsoil 10^{-8} m^{3}kg^{-1}	χ_{hf} topsoil 10^{-8} m^{3}kg^{-1}	κ_{is} 10^{-5} SI	Clay %	Silt %	Sand %
Median	36.0	32.3	31.1	27.5	34.0	23.7	63.5	11.2
Mean	34.9	31.4	30.3	27.0	34.0	23.5	59.2	17.2
SD	9.6	8.6	8.3	7.3	11.6	9.1	13.7	17.4
Min	16.0	14.7	13.9	12.7	13.3	4.9	17.9	1.8
Max	57.6	53.3	46.0	41.0	64.0	68.3	73.8	77.2

the measuring position, the magnetic field was 500 mT and was measured using a Hall effect magnetometer. The temperature was controlled and the force recorded with a sensor that generates an output voltage. Such voltage is acquired using a PicoLog® recorder. In this study, the relative values of induced magnetization (M/M_{RT}) are of interest; hence the M/M_{RT}–T curves are presented. Measurements were performed in air. Each sample was heated to a temperature of about 700 °C and subsequently cooled to room temperature (RT) with a controlled heating/cooling rate of 30 °C min^{-1}.

3 RESULTS AND DISCUSSION

3.1 Spatial distribution of magnetic susceptibility and its relationship with landscape and soil properties

The results of mass specific and volumetric magnetic susceptibility measured on bulk and topsoil samples in the laboratory and in the field respectively are presented in Table 1. Values of mass magnetic susceptibility measured at low frequency (χ_{lf}) were always higher than those at high frequency (χ_{hf}). The median of χ_{lf} in bulk core samples was slightly higher and significantly different ($p < 0.05$) to that in the topsoil samples.

A high correlation was found between the χ_{lf} values in the bulk core samples and the χ_{lf} in the topsoil samples ($r = 0.951, p < 0.01$). Similarly high correlations were found between χ_{lf} in bulk and topsoil samples in the laboratory and κ_{is} in the field ($r = 0.891$, $r = 0.894$, $p < 0.01$, respectively).

The magnetic susceptibility measurements displayed similar general trends and spatial variability patterns (Fig. 2). The highest χ_{lf} values in bulk and topsoil samples were recorded in the upper part of the field, said values decreasing towards the bottom part. A similar spatial distribution was observed for κ_{is} data. Therefore, in agreement with (Schibler *et al.* 2002), *in situ* measurements in the field using the MS2D probe is a suitable tool to screen the magnetic susceptibility of soils. These results are relevant especially in non-polluted areas with a relatively low magnetic signal where measurements of κ_{is} can be used as a quick and effective method to obtain a preliminary reference of the spatial distribution of the magnetic minerals in soil surface layers.

The physiographic characteristics of the study area, elevation and slope determine the water flow lines (Fig. 3). In the convergence flow areas at the bottom part with lower elevation values, there were lower clay and silt contents (Fig. 3), unlike the divergence areas where the clay content was higher. Alba (2003) also found, in cultivated soils, that the distribution of soil texture was influenced by run-off.

The gully system draining the hydrological unit is a main driver of the soil redistribution processes. The upper part is an interrill area that maintains more stable soil conditions and is not incised by the gully that starts below this divergence area. Soil erosion by run-off intensifies downslope, in the middle and lower parts of the field triggering the removal of soil particles, including magnetic minerals. The water flow pathway determines the distribution of the size of soil particles within the study field. At the lower end of the gully there is deposition of coarse soil particles whereas finer particles are exported out of the field to the main ephemeral stream.

Similar results were found when comparing the Pearson's correlation coefficients for the additive log-ratio untransformed and transformed soil texture data but less significant correlations were found when using the additive log-ratio transformation. Therefore, untransformed soil texture data are presented in this study.

Mass specific and volumetric magnetic susceptibility are directly correlated with the percentage of clay and silt (Table 2) but they are inversely correlated with the percentage of sand, suggesting that magnetic minerals are associated with finer soil particles. Thompson & Morton (1979) found that for a given parent material low magnetic susceptibility values are related to a high content of coarse

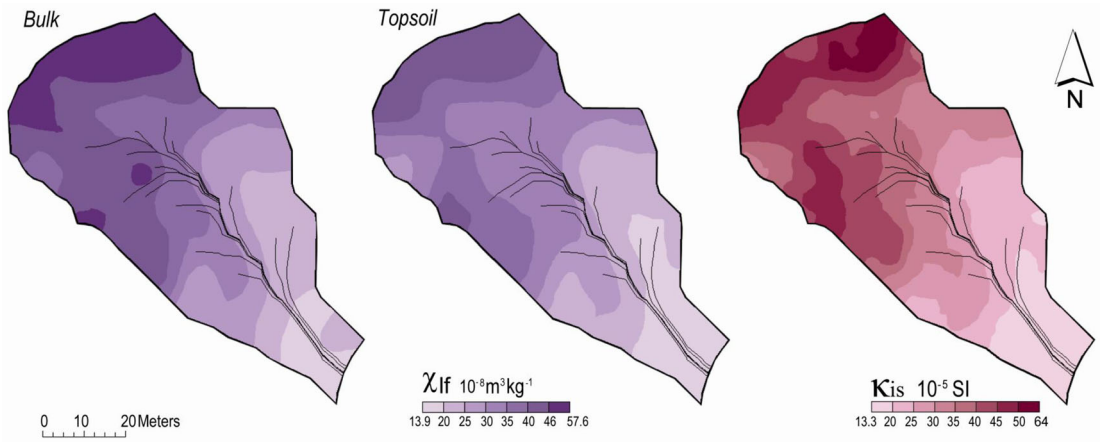

Figure 2. Maps of mass specific magnetic susceptibility at low frequency in bulk and topsoil samples measured in the laboratory and volumetric magnetic susceptibility measured in the field (κ_{is}).

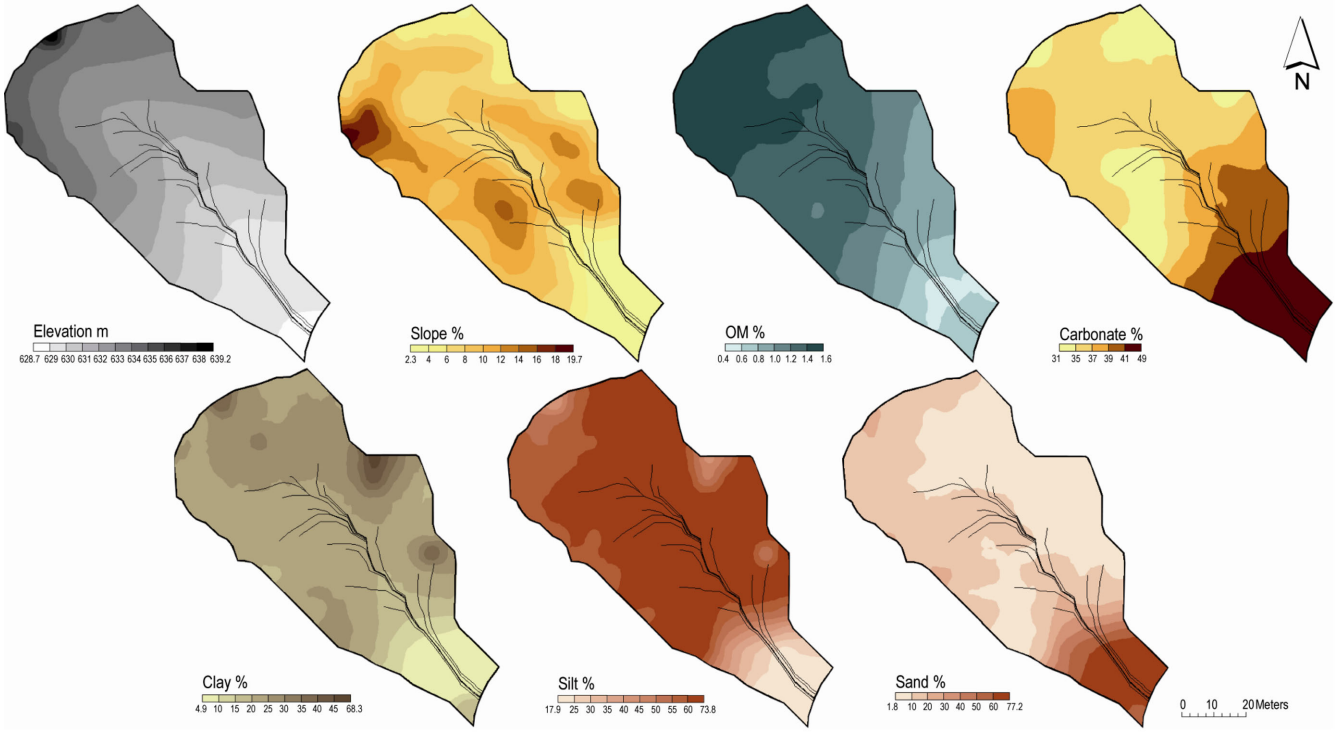

Figure 3. Maps of soil properties (elevation, slope, organic matter, carbonate contents and soil texture).

Table 2. Pearson's coefficients ($n = 154$).

	χ_{lf} bulk	χ_{lf} topsoil	κ_{is}	Clay	Silt	Sand	Elevation
χ_{lf} topsoil	0.951[a]						
κ_{is}	0.891[a]	0.894[a]					
Clay	0.268[a]	0.308[a]	0.227[a]				
Silt	0.339[a]	0.342[a]	0.355[a]	0.122			
Sand	−0.408[a]	−0.399[a]	−0.399[a]	−0.623[a]	−0.852[a]		
Elevation	0.825[a]	0.828[a]	0.768[a]	0.443[a]	0.319[a]	−0.485[a]	
Slope	0.408[a]	0.435[a]	0.376[a]	0.252[a]	0.096	−0.208[a]	0.599[a]

[a]Correlation is significant at 0.01 level.

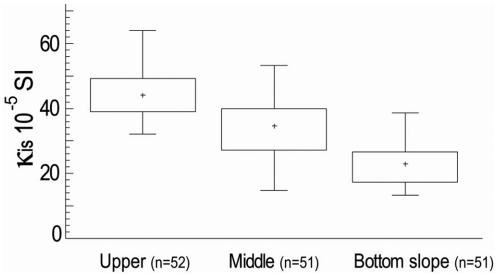

Figure 4. Box plot of the volumetric magnetic susceptibility measured in the field in different slope positions.

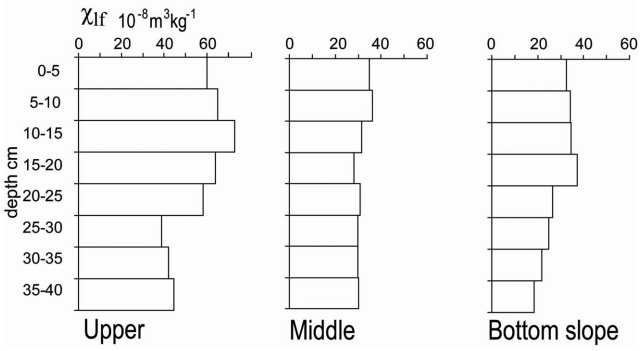

Figure 5. Soil depth profiles at three different slope locations.

particles whereas high magnetic susceptibility values correspond to finer soil particles in lake sediments. According to Alekseev *et al.* (2002), in soils developed from parent material with low magnetic susceptibility values such as that of the study field, the highest values of magnetic susceptibility are correlated with the clay fraction content (<0.002 mm). Magnetic susceptibility progressively decreases in silt and sand fractions, the former being the most abundant and homogeneously distributed in the study area (Table 2, Fig. 3). The mean values of κ_{is} obtained at different slope positions are significantly different ($p < 0.05$) (Fig. 4). The three depth soil profiles of χ_{lf} taken along the slope confirmed this trend (Fig. 5).

The relationship of elevation and slope with the mass specific and volumetric magnetic susceptibility values were direct and statistically significant (Table 2). The highest magnetic susceptibility values were found at upslope positions where clay and organic matter contents were also more abundant. Williams & Cooper (1990) also found high values of magnetic susceptibility at upslope positions in a natural prairie field. Contrary to this, the lowest mass specific and volumetric magnetic susceptibility values were at downslope positions coinciding with higher sand and carbonate contents and

Table 3. Pearson's coefficients ($n = 40$).

	χ_{lf} bulk	χ_{lf} topsoil	κ_{is}	Clay	Silt	Sand	OM	$CaCO_3$	Elevation
χ_{lf} topsoil	0.977[a]								
κ_{is}	0.905[a]	0.909[a]							
Clay	0.379[b]	0.401[b]	0.361[b]						
Silt	0.437[a]	0.454[a]	0.447[a]	0.759[a]					
Sand	−0.443[a]	−0.462[a]	−0.445[a]	−0.875[a]	−0.979[a]				
OM	0.811[a]	0.800[a]	0.727[a]	0.594[a]	0.675[a]	−0.687[a]			
$CaCO_3$	−0.676[a]	−0.709[a]	−0.673[a]	−0.701[a]	−0.625[a]	0.683[a]	−0.662[a]		
Elevation	0.865[a]	0.874[a]	0.820[a]	0.573[a]	0.534[a]	−0.575[a]	0.827[a]	−0.696[a]	
Slope	0.440[a]	0.458[a]	0.482[a]	0.123	0.231	−0.210	0.533[a]	−0.339[b]	0.553[a]

[a]Correlation is significant at 0.01 level.
[b]Significant at 0.05 level.

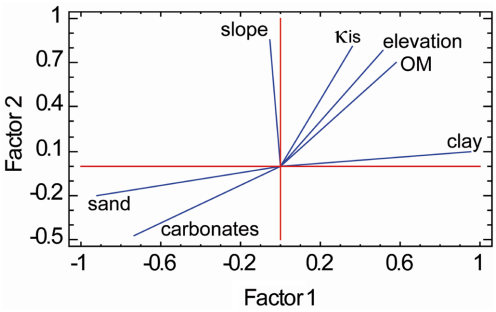

Figure 6. Biplot of the factor analysis.

lower organic matter contents (Fig. 3). This was further confirmed by the direct and high correlation between magnetic susceptibility and organic matter and the inverse relationships with carbonate contents (Table 3). Carbonates, in particular, calcite has diamagnetic properties, hence its magnetic susceptibility is negative (Hunt *et al.* 1995; Dearing 1999). Although it cannot be generalized, higher contents of calcite ($CaCO_3$) may yield a decrease of magnetic susceptibility as it is observed in our study case. Therefore, the main controls of the spatial variability of magnetic susceptibility are those related to soil redistribution processes by water erosion through the gully system that also influences the spatial variability of the other soil components.

Topographic factors are linked to soil drainage, translocation of soil particles and the concentration of magnetic minerals in soils. The factor analysis identified two main factors which explain 82.2 per cent of data variance. Volumetric magnetic susceptibility, clay, organic matter and elevation were grouped together and their distribution was the opposite of that of the sand and carbonates contents (Fig. 6). These results support the links observed in the study field and could be the base to describe the relationships between the spatial pattern of magnetic properties, topographic and soil parameters for a similar cultivated landscape.

3.2 Magnetic enhancement and soil magnetic mineralogy

Results of magnetic concentration (χ, ARM, χ_{ARM} and SIRM), mineralogy (H_{CR}, *S*-ratio and SIRM/κ) and grain size (χ_{fd}%, κ_{ARM}/κ-ratio, SIRM/κ and ARM/SIRM) dependent parameters are displayed in Table 4.

Concentration-related parameters also display variations in the study area, as well as in depth with higher values of χ, ARM and SIRM at 30 cm than at 50 cm. Values of χ ranged from 13.7 to 47.6 $\times$ 10^{-8} m^3 kg^{-1}. The mean of magnetic susceptibility at 30 cm depth is higher (39.2 $\times$ 10^{-8} m^3 kg^{-1}) and statistically different from the mean of magnetic susceptibility at 50 cm depth (21 $\times$ 10^{-8} m^3 kg^{-1}).

The χ increase in the 30 cm samples with regard to the 50 cm samples is related to the slope position. The depth profiles collected along the slope show that χ is higher at the upper slope than at the bottom slope positions (Fig. 5). Most of the 50 cm soil samples are located at the bottom slope where runoff exports the fine soil components out of the field, thus decreasing the magnetic minerals which are preferentially accumulated in the clay fraction (Fine *et al.* 1989, 1993). In addition, a slight decrease of magnetic susceptibility values with depth is observed (Fig. 5). The decrease below the plough layer (25–30 cm) was more evident in the upper and bottom slope profiles. These profiles show magnetic increases of about 50–80 per cent suggesting that agricultural practices influence the vertical distribution of magnetic minerals by mixing the upper soil layers. Tillage practices improve aeration and increase water infiltration favouring conditions for the neoformation of nanosized magnetic minerals (magnetite/maghemite) in the upper soil layers.

Measurements of remanent magnetization and its magnetic parameters (H_{CR} and *S*-ratio) suggest that the magnetic signal is controlled by a magnetite-like phase and or maghemite (Table 4). The *S*-ratio values (between 0.785 and 0.921) clearly show the predominance of ferrimagnetic minerals (*S*-ratio ∼1) over antiferromagnetic minerals (*S*-ratio ∼ −1). Furthermore, the values of H_{CR} range from 19.9 to 25.2 mT, as can be observed in Table 4, which is in agreement with characteristic values of magnetite and maghemite (Peters & Dekkers 2003). H_{CR} varies only slightly, indicating a similar magnetic mineralogy for these soil samples.

The IRM acquisition measurements show the dominance of ferrimagnetic minerals. However, a subordinate contribution of high coercivity minerals is evident in these measurements; most of the curves do not reach their saturation at 300 mT. As appreciated in Fig. 7, most of the selected samples evidenced an additional (higher coercivity) magnetic phase. Such a phase can correspond to the presence of other magnetic minerals such as hematite and/or goethite.

The presence of antiferromagnetic minerals such as hematite can be determined from separation methods of IRM acquisition and backfield (Chaparro *et al.* 2005). According to the Chaparro´s method, the presence of subordinate magnetic phases is detected and semi-quantified for 30 selected samples (Table 4). The contribution of these phases to the total IRM (backfield) is between 6.7 and 12.6 per cent with H_{CR} values of 553.5–711.6 mT, which are indicative of hematite minerals (Fig. 8). Although the presence of goethite is not ruled out, this mineral seems to present higher values of H_{CR} (Peters & Dekkers 2003). In Table 4, the dominance of low coercivity phases can be observed, for example phase contribution of magnetite/maghemite is about 90 per cent, in the three main

Table 4. Magnetic concentration and mineral-dependent parameters of samples from Upper (37825–37905), Middle (38037–38400) and Bottom (38334–38359) slope positions. Separation of magnetic phases from Chaparro *et al.* (2005).

Samples	Depth (cm)	χ (10^{-8} m^3 kg^{-1})	ARM (10^{-6} A m^3 kg^{-1})	SIRM [10^{-3} A m^2 kg^{-1})	χ_{fd} (%)	χ_{fd} (10^{-9} m^3 kg^{-1})	κ_{ARM}/κ (dimensionless)	ARM/SIRM (dimensionless)	SIRM/κ (kA m^{-1})	H_{CR} (mT)	*S*-ratio (dimensionless)	Phase1 (%)	Phase2 (%)	H_{CR}1 (mT)	H_{CR}2 (mT)	*S*-ratio1 (dimensionless)	*S*-ratio2 (dimensionless)
37825	30	43.9	191.7	3.1	10.90	52.0	6.31	0.063	6.99	23.7	0.84	91.30	8.70	21.6	576.0	0.98	− 0.30
37826	30	47.2	189.4	3.4	9.39	48.0	5.78	0.055	7.30	22.6	0.86	92.40	7.60	20.9	587.2	0.98	− 0.32
37832	31	43.8	211.7	2.9	10.61	49.0	6.96	0.072	6.73	23.9	0.83	91.80	8.30	22.3	577.3	0.93	− 0.26
37833	30	40.4	198.3	2.7	9.01	40.0	7.05	0.074	6.65	23.4	0.87	92.26	7.74	21.7	576.2	0.97	− 0.30
37834	32	47.5	210.5	3.6	9.28	49.0	6.40	0.058	7.64	23.0	0.90	93.30	6.70	21.5	574.6	0.99	− 0.30
37853	30	43.0	201.7	2.8	10.15	46.0	6.75	0.072	6.51	19.9	0.92	93.00	7.00	20.0	563.4	0.98	− 0.27
37854	31	42.7	202.3	2.7	10.55	48.0	6.82	0.074	6.42	23.3	0.84	92.70	7.30	21.4	596.8	0.96	− 0.32
37877	30	45.0	206.0	2.9	9.98	47.0	6.59	0.072	6.38	22.5	0.87	92.51	7.49	21.0	553.5	0.96	− 0.29
37878	30	45.6	216.6	3.2	12.45	61.0	6.61	0.069	6.92	24.2	0.87	93.10	6.90	22.5	566.2	0.98	− 0.29
37905	30	47.6	223.9	3.1	10.96	55.0	6.76	0.073	6.47	22.5	0.86	92.60	7.40	20.9	610.8	0.97	− 0.31
Mean		*44.7*	*205.2*	*3.0*	*10.33*	*49.5*	*6.60*	*0.068*	*6.80*	*22.9*		*92.50*	*7.51*	*21.4*	*578.2*		
SD		*2.4*	*10.8*	*0.3*	*1.01*	*5.6*	*0.37*	*0.007*	*0.41*	*1.2*		*0.61*	*0.62*	*0.7*	*16.6*		
38037	30	35.9	173.0	2.4	10.41	41.0	6.90	0.073	6.63	23.7	0.85	90.15	9.85	21.7	579.2	0.97	− 0.25
38038	30	35.4	159.5	2.3	10.00	38.0	6.50	0.068	6.63	23.5	0.83	91.40	8.60	21.4	603.0	0.97	− 0.30
38039	30	31.4	150.9	2.1	9.94	33.0	6.84	0.072	6.66	24.9	0.83	89.66	10.43	22.5	586.0	0.95	− 0.25
38051	30	34.0	167.1	2.3	10.61	38.0	7.05	0.073	6.76	23.8	0.82	91.80	8.20	22.1	579.8	0.92	− 0.28
38108	30	29.1	153.9	2.0	10.54	33.0	7.54	0.077	6.88	23.9	0.81	90.70	9.30	22.3	588.7	0.91	− 0.27
38109	30	26.2	138.8	1.9	9.43	28.0	7.60	0.073	7.22	24.0	0.84	88.07	11.93	21.7	569.9	0.99	− 0.26
38138	30	28.5	142.1	2.1	11.18	34.0	7.13	0.068	7.31	24.4	0.82	90.10	9.90	21.9	661.8	0.94	− 0.32
38394	50	35.2	166.3	2.3	11.02	41.0	6.80	0.073	6.50	22.1	0.84	91.30	8.70	20.1	605.5	0.94	− 0.28
38399	50	30.8	148.6	2.3	11.69	38.0	6.95	0.065	7.37	25.2	0.83	89.50	10.50	23.0	611.0	0.92	− 0.25
38400	50	33.2	161.0	2.2	10.96	40.0	6.96	0.073	6.65	22.6	0.84	89.50	10.50	20.2	654.0	0.96	− 0.28
Mean		*32.0*	*156.1*	*2.2*	*10.58*	*36.4*	*7.03*	*0.071*	*6.86*	*23.8*		*90.22*	*9.79*	*21.7*	*603.9*		
SD		*3.3*	*11.2*	*0.2*	*0.67*	*4.2*	*0.33*	*0.003*	*0.32*	*0.9*		*1.12*	*1.12*	*0.9*	*31.3*		
38334	50	18.3	84.8	1.4	8.50	17.0	6.62	0.060	7.74	23.2	0.83	88.40	11.60	20.2	697.1	0.91	− 0.38
38335	50	21.9	73.5	1.7	7.96	16.0	4.81	0.043	7.83	22.1	0.83	92.47	7.53	20.5	639.6	0.93	− 0.44
38345	49	17.1	66.3	1.4	7.89	15.0	5.53	0.047	8.28	22.9	0.81	88.30	11.70	20.2	710.3	0.97	− 0.42
38346	50	16.6	58.1	1.4	6.70	13.0	5.03	0.041	8.62	22.2	0.81	89.30	10.70	19.7	686.5	0.94	− 0.34
38347	50	16.0	53.6	1.3	9.52	18.0	4.74	0.040	8.36	23.3	0.79	87.40	12.60	20.3	711.6	0.93	− 0.35
38348	50	15.4	52.8	1.3	7.14	13.0	4.90	0.039	8.66	23.0	0.80	89.90	10.10	20.7	700.0	0.92	− 0.41
38356	50	18.2	58.6	1.6	9.55	19.0	4.51	0.037	8.74	22.7	0.79	90.60	9.40	21.0	670.6	0.91	− 0.38
38357	50	19.1	58.2	1.6	5.80	13.0	4.30	0.035	8.62	21.9	0.83	90.70	9.30	19.4	703.9	0.94	− 0.38
38358	50	17.4	57.0	1.4	7.25	14.0	4.65	0.040	8.19	22.7	0.80	89.68	10.32	21.0	632.7	0.93	− 0.33
38359	50	13.7	53.1	1.2	8.13	13.0	5.47	0.044	8.90	23.4	0.79	90.84	9.16	21.6	614.2	0.91	− 0.40
Mean		*17.4*	*61.6*	*1.5*	*7.84*	*15.1*	*5.06*	*0.043*	*8.39*	*22.8*		*89.76*	*10.24*	*20.5*	*676.6*		
SD		*2.2*	*10.4*	*0.2*	*1.18*	*2.3*	*0.67*	*0.007*	*0.39*	*0.5*		*1.49*	*1.49*	*0.7*	*35.6*		

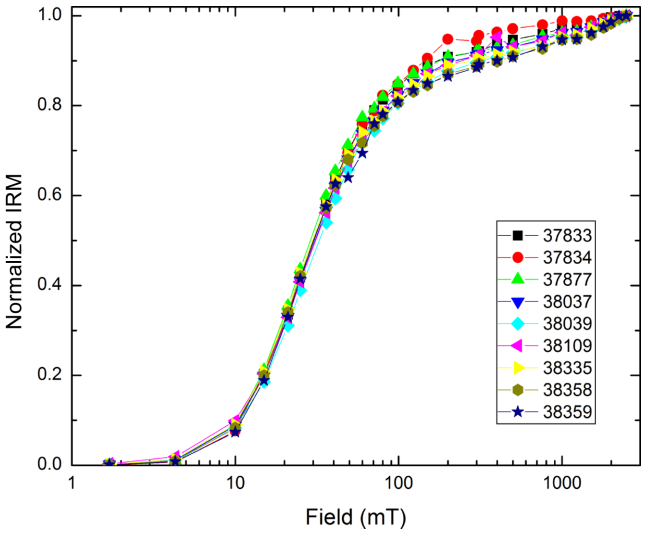

Figure 7. Measurements of acquisition IRM for selected samples. A main ferrimagnetic phase and a subordinate contribution of high coercivity minerals are observed.

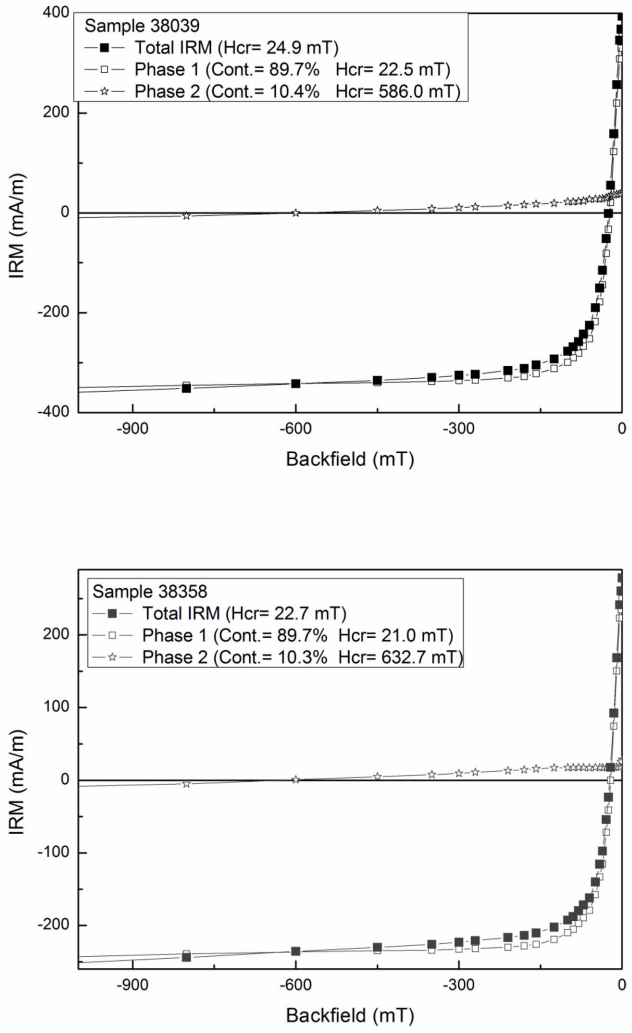

Figure 8. Separation of IRM backfield measurements into two phases using a new experimental method (Chaparro *et al.* 2005). For each sample, curves of Total back IRM (without AF filter) and achieved phases are shown. The contribution of subordinate (high coercivity) magnetic phases can be observed.

topographic areas. However, it is also possible to see a decreasing (in contribution) pattern of the low coercivity phase as opposed to the high coercivity phase from upslope to downslope areas (see mean values in Table 4). It is worth mentioning that the percentages (contribution of phases) represent the contribution to remanent magnetization and they are not directly related to the weight concentration of magnetic materials. For example, Chaparro & Sinito (2004) found percentages of high coercivity phases of ∼33 and 65 per cent for mixed samples containing 99.1 and 99.8 per cent (110:1 and 420:1 hematite:magnetite) of hematite, respectively. The signal dominance of magnetite over hematite is a consequence of its concentration-dependent magnetic parameters, and similar results were obtained for detailed studies carried out by Frank & Nowaczyk (2008).

Thermomagnetic curves of representative samples from different topographic position are shown in Fig. 9. Most of the samples have Curie temperatures closer to that of magnetite ($T_c = 580$ °C), however, above this characteristic temperature, a high coercivity phase is also evident. The heating runs show systematic $M(T)$ changes starting at about 420–430 °C for all the samples, which supports the previous findings of high coercivity magnetic phases. These changes were previously observed and reported by Hanesch *et al.* (2006) in synthetic, ore and soil samples containing hematite/goethite and organic carbon. As reported, the presence of organic carbon in samples leads to reducing conditions and promotes the neoformation of ferrimagnetic phases; in this study, magnetite-like phases with Curie temperatures of 500–550 °C are observed in the cooling runs. It is worth mentioning that the sample 38 358 shows a moderate change in the heating and the cooling runs, which may be related to the lower organic matter content (0.4–0.6 per cent) in this downslope position (see Fig. 3).

Magnetite formation typically involves biomineralization by iron-reducing bacteria which gain energy through the oxidation of organic matter (Guo & Barnard 2013). Hematite may form by the weathering of Fe-bearing lithogenic minerals (Chen *et al.* 2010; Torrent *et al.* 2010b). The formation of hematite, which is common in Mediterranean soils (Torrent & Barrón 2002) is favoured by warm temperatures and low organic matter contents that are typical environmental conditions in the study field.

Values of κ_{ARM} and κ for all samples are displayed in the King's plot (Fig. 10), and suggest the occurrence of magnetic grain sizes below 0.1 μm. Moreover, two groups are observed for samples at 30 cm (upper part) and at 50 cm (lower part, in grey).

The changes in magnetic grain size seem to be in agreement with the concentration trend. For example, higher concentrations coincide with a higher κ_{ARM}/κ-ratio and ARM/SIRM (positive significant correlations, Table 5), and vice versa, hence changes in concentration are accompanied by the presence of finer (coarser) magnetic grains. Values of SIRM/χ, from 5.9 to 8.3 kA m^{-1}, belong to the range of magnetite and lower values are interpreted as an abundance of finer magnetic grain sizes. This interpretation, according to Peters & Dekkers (2003), is based on the fact that there are magnetite grains of less than 1 μm. This is also supported by the significant negative correlation between SIRM/χ and κ_{ARM}/κ-ratio, and ARM/SIRM (Table 5). The trend can also be observed in Fig. 11(a).

The presence of ultrafine (<0.03 μm) SP minerals was estimated from the percentage frequency dependent susceptibility (χ_{fd}%) measured in the laboratory. In Table 4 it is possible to note values

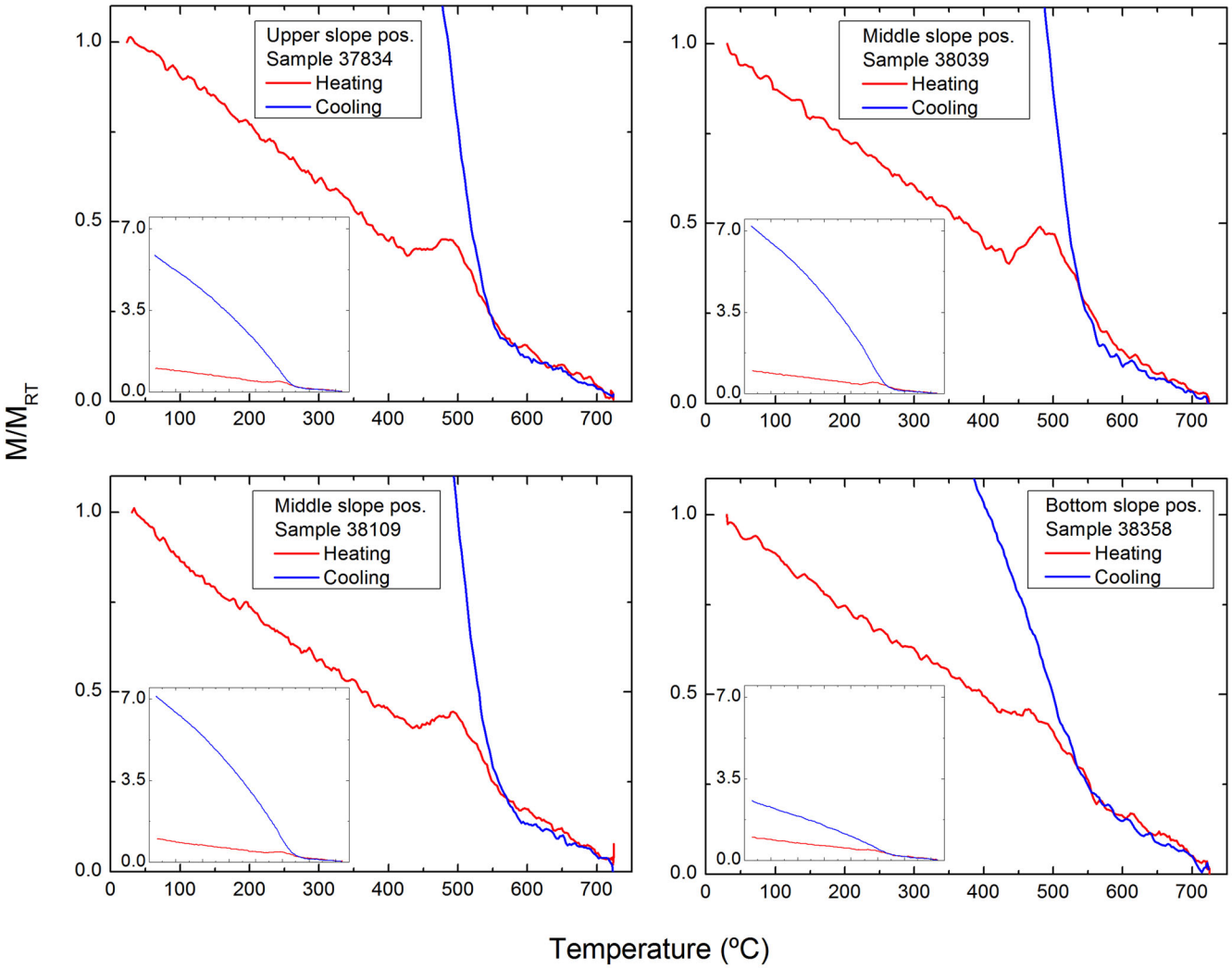

Figure 9. Thermomagnetic measurements of 4 soil samples at three different slope positions. The Curie temperatures correspond to magnetite and to a high coercivity phase. It is evident a magnetic change at about 420 °C associated to a high coercivity phase of hematite/goethite. In addition, there is a noticeable difference between the magnetic changes in the cooling curves (inset graphs).

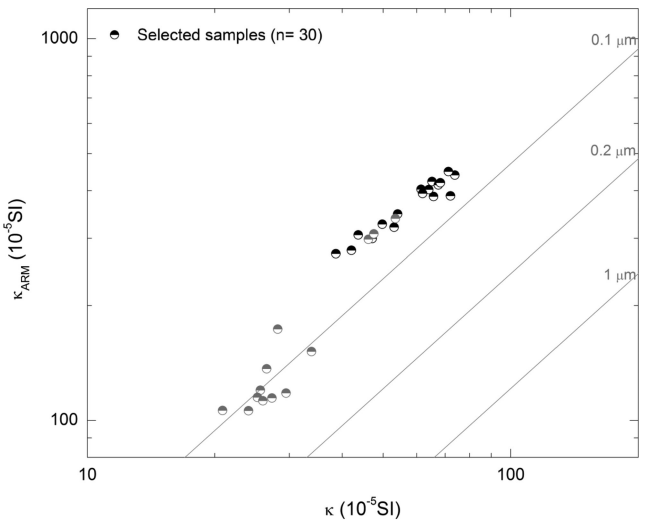

Figure 10. King's plot (κ_{ARM} versus κ) for selected samples. Two grouping are observed: samples at 30 cm (upper part) and at 50 cm (lower part, in grey colour).

of χ_{fd}% between 5.8 and 12.4 per cent, which are indicative of the presence and dominance of SP grains (Dearing *et al.* 1996). Values of χ_{fd}% < 5 per cent are typical of samples in which non-SP grains dominate or where extremely fine grains (<0.005 μm) dominate the SP fraction (Dearing 1999). This parameter correlates statistically with sensitive grain size dependent parameters κ_{ARM}/κ-ratio and ARM/SIRM (Table 5, Figs 11b and c).

Dearing (1999) established that samples with high values of χ_{fd}% ranging from 10 to 14 per cent can be interpreted as soils in which virtually all iron components are SP grains (>75 per cent). Therefore, χ_{fd}% can be used semi-quantitatively to estimate the concentration of SP grains.

Most of the 30 cm samples located at upper and middle slope positions show high χ_{fd}% values (Table 4). However, the 50 cm samples at bottom positions had χ_{fd}% values lower than 10 per cent indicating concentration of SP grains lower than 75 per cent. The higher concentration of SP in the 30 cm samples than in the 50 cm samples could be associated with '*in situ*' formation of SP under oxidizing conditions in the plough layer favored by tillage. Moreover tillage also promotes soil physical disruption that may disaggregate large magnetic mineral grains into smaller ones thus producing higher amounts of SP particles (Maher 1998).

Table 5. Pearson's coefficients ($n = 30$).

	χ	ARM	SIRM	χ_{ARM}	κ_{ARM}/κ	ARM/SIRM	SIRM/κ	H_{CR}
ARM	0.976[a]							
SIRM	0.980[a]	0.932[a]						
χARM	0.977[a]	0.999[a]	0.932[a]					
κARM/κ	0.616[a]	0.764[a]	0.521[a]	0.764[a]				
ARM/SIRM	0.721[a]	0.846[a]	0.607[a]	0.846[a]	0.966[a]			
SIRM/κ	−0.819[a]	−0.888[a]	−0.702[a]	−0.889[a]	−0.831[a]	−0.941[a]		
H_{CR}	0.013	0.110	0.010	0.110	0.389[b]	0.280	−0.120	
Sratio	0.798[a]	0.766[a]	0.801[a]	0.767[a]	0.457[b]	0.529[a]	−0.612[a]	−0.340

[a]Correlation is significant at 0.01 level.
[b]Significant at 0.05 level.

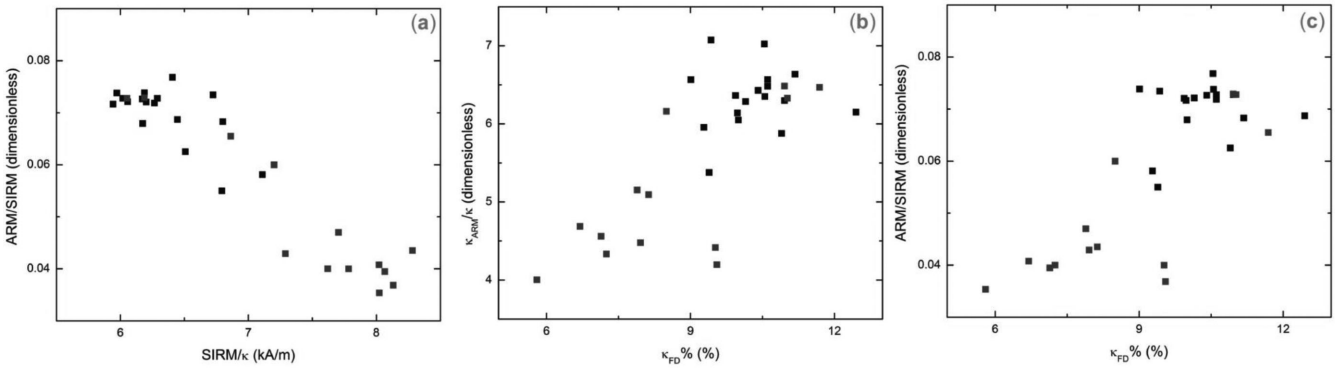

Figure 11. Biplot of (a) ARM/SIRM versus SIRM/κ, (b) κ_{ARM}/κ versus κ_{FD}% and (c) ARM/SIRM versus κ_{FD}% for selected samples.

Moreover, the lateral distribution of SP grains showed a decreasing concentration from upper to bottom slope positions, as indicated by the mean values of χ_{fd} that vary from 49.5, 36.4 and 15.1 $\times 10^{-9}$ m^3 kg^{-1} at upper, middle and bottom slope positions, respectively (Table 4). In agreement with Suchodoletz *et al.* (2009) magnetic properties depend largely on the grain size distribution of the particles being the magnetic susceptibility largest for ultraffine SP particles. At the bottom part of the slope the selective loss of fine fractions transported by run-off and the consequent removal of the ultrafine SP grains contained in the clay size fraction is related with lower χ_{fd}.

Furthermore, the pedogenic fine-grained ferromagnetic particles decreased with depth. In topsoil samples (5 cm) χ_{fd}% values varied from 6.1 to 13.1 per cent, in 30 cm samples χ_{fd}% values ranged from 5.0 to 13.3 per cent and in 50 cm samples χ_{fd}% values were between 5.8 and 11.7 per cent. The means of χ_{fd}% values in 5, 30 and 50 cm soil samples were 10.7, 10.1 and 9.0 per cent, respectively and there was a statistically significant difference between them ($p < 0.05$). In topsoil samples, 76 per cent of χ_{fd}% values ranged from 10 to 13.1 per cent whereas in the bulk samples, 53 per cent of the samples ranged from 10 to 13.3 per cent, suggesting that topsoils have higher concentrations of SP minerals than bulk core samples. Therefore, frequency dependent susceptibility seems to be a useful parameter to infer the abundance of pedogenic fine-grained ferromagnetic particles.

4 CONCLUSIONS

The spatial variation in the distribution of the magnetic parameters in the agricultural Calcisols studied provided the basis for assessing the relationships between soil redistribution processes and soil magnetic properties in cultivated Mediterranean fields.

The analysis of the topographic characteristics defining the soil redistribution through the drainage flow pattern, the spatial variability of magnetic parameters and soil properties such as soil texture, organic matter and carbonate content, supported the relationships between the magnetic minerals, finer soil particles and the organic matter content, suggesting that erosion by runoff determines the pattern of soil redistribution (erosion and deposition) in the field, being the main cause for the spatial variability of magnetic minerals through removal of fine soil components.

The depth distribution of magnetic minerals is influenced by tillage practices that mix the soil thoroughly improving aeration and increasing water infiltration, thereby favouring conditions for the neoformation of nanosized magnetic minerals (magnetite) in the upper soil layers.

The presence of pedogenic magnetic minerals such as magnetite and hematite is associated with soil formation conditions. These minerals were detected by thermomagnetic measurements and the dominance of magnetite over hematite was semi-quantitatively estimated via an experimental method of magnetic phase separation in which the phase contribution of magnetite was found to be approximately 90 per cent to the Total SIRM. Although there are slight changes in magnetic mineralogy, there is a discernible decreasing pattern (in terms of contribution) in the low coercivity phase (magnetite) from upslope to downslope. SP minerals are found to decrease with depth suggesting an enrichment of pedogenic minerals in the upper soil layers favoured by soil conditions within the plough layer. In addition, preferential areas of preservation of SP grains are found, with lower concentration of SP grains observed at downslope positions, likely associated with the erosion processes.

In situ magnetic susceptibility measurements of topsoils have been proved a useful tool for screening the contents of magnetic minerals in cultivated soils with low magnetic signal. The distribution patterns of soil magnetic properties in combination with

physiographic and edaphic parameters are meaningful indicators of soil condition and can provide useful information on soil processes in Mediterranean agroecosystems.

ACKNOWLEDGEMENTS

This work was funded by the CICYT project EROMED (CGL2011–25486). The authors thank the Universidad Nacional del Centro de la Provincia de Buenos Aires (UNCPBA), and the National Council for Scientific and Technological Research (CONICET). The authors also thank to Dr Harald Böhnel and Ing. Jorge Escalante for valuable support to carry out additional studies in their Paleomagnetic Laboratory (CGEO-UNAM). The authors thank to Dr Kapicka and an anonymous reviewer for their fruitful suggestions as well.

REFERENCES

Aitchison, J., 1982. The statistical analysis of compositional data, *J. R. Stat. Soc., Ser. B (Stat. Methodol.)*, **44**(2), 139–177.

Aitchison, J., 1986. The statistical analysis of compositional data, in *Monographs on Statistics and Applied Probability,* Chapman & Hall Ltd., 416 pp.

Alba, S. de, 2003. Simulating long-term soil redistribution generated by different patterns of moldboard ploughing in landscapes of complex topography, *Soil Tillage Res.,* **71**(1), 71–86.

Alekseev, A., Alekseeva, T., Sokolowska, Z. & Hajnos, M., 2002. Magnetic and mineralogical properties of different granulometric fractions in the soils of the Lublin Upland Region, *International Agrophysics,* **16,** 1–6.

Bartington Instruments Ltd., 2000. *Operation manual for MS2 Magnetic Susceptibility System,* Bartington Instruments Ltd, pp. 72.

Bidegain, J.C., Rico, Y., Bartel, A., Chaparro, M.A.E. & Jurado, S., 2009. Magnetic parameters reflecting pedogenesis in Pleistocene loess deposits of Argentina, *Quarter. Int.,* **209,** 175–186.

Blundell, A., Hannam, J.A., Dearing, J.A. & Boyle, J.F., 2009. Detecting atmospheric pollution in surface soils using magnetic measurements: a reappraisal using an England and Wales database, *Environ. Pollut.,* **157,** 2878–2890.

Chaparro, M.A.E. & Sinito, A.M., 2004. An alternative experimental method to discriminate magnetic phases using IRM acquisition curves and magnetic demagnetisation by alternating field, *Revista Brasileira de Geofisica,* **22**(1), 17–32.

Chaparro, M.A.E., Lirio, J.M., Nuñez, H., Gogorza, C.S.G. & Sinito, A.M., 2005. Preliminary magnetic studies of lagoon and stream sediments from Chascomus Area (Argentina)—magnetic parameters as indicators of heavy metal pollution and some results of using an experimental method to separate magnetic phases, *Environ. Geol.,* **49,** 30–43.

Chaparro, M.A.E., Gogorza, C.S.G., Chaparro, M.A.E., Irurzun, M.A. & Sinito, A.M., 2006. Review of magnetism and heavy metal pollution studies of various environments in Argentina, *Earth Planets Space,* **58**(10), 1411–1422.

Chaparro, M.A.E., Nuñez, H., Lirio, J.M., Gogorza, C.S.G. & Sinito, A.M., 2007. Magnetic screening and heavy metal pollution studies in soils from Marambio station, Antarctica, *Antarctic Sci.,* **19,** 379–393.

Chaparro, M.A.E., Marié, D.C., Gogorza, C.S.G., Navas, A. & Sinito, A.M., 2010. Magnetic studies and scanning electron microscopy X-ray energy dispersive spectroscopy analyses of road sediments, soils, and vehicle-derived emissions, *Stud. Geophys. Geod.,* **54**(4), 633–650.

Chen, T., Xie, Q., Xu, H., Chen, J., Ji, J., Lu, H. & Balsam, W., 2010. Characteristics and formation mechanism of pedogenic hematite in Quaternary Chinese loess and paleosols, *Catena,* **81,** 217–225.

Collinson, D.W., 1983. *Methods in Rock Magnetism and Palaeomagnetism: Techniques and Instrumentation,* Chapman & Hall.

CSIC, Consejo Superior de Investigaciones Científicas, 1976. Comisión de métodos analíticos, *Anales Edafología y Agrobiología,* **35,** 813–814.

Dearing, J., 1999. Environmental magnetic susceptibility, *Using the Bartington MS2 System,* 2nd edn, Chi Publishing, 54 pp.

Dearing, J.A., Dann, R.J.L., Hay, K., Lees, J.A., Loveland, B.A., Maher, B.A. & O'Grady, K., 1996. Frequency-dependent susceptibility measurements of environmental materials, *Geophys. J. Int.,* **124,** 228–240.

Dearing, J.A., Bird, P.M., Dann, R.J.L. & Benjamin, S.F., 1997. Secondary ferrimagnetic minerals in Welsh soils: a comparison of mineral magnetic detection methods and implications for mineral formation, *Geophys. J. Int.,* **130,** 727–736.

Escalante, J.E. & Böhnel, H.N., 2011. Diseño y Construcción de una Balanza de Curie [*Design and construction of a Curie Balance*], *Geos,* **31**(1), 63.

Evans, M.E. & Heller, F., 2003. *Environmental Magnetism; Principles and Applications of Enviromagnetics,* Academic Press, pp. 299.

Fine, P., Singer, M.J., La Ven, R., Verosub, K. & Southard, R.J., 1989. Role of pedogenesis in distribution of magnetic susceptibility in two California chronosequences, *Geoderma,* **44,** 287–306.

Fine, P., Singer, M.J., Verosub, K.L. & TenPas, J., 1993. New evidence for the origin of ferimagnetic minerals in loess from China, *Soil Sci. Soc. Am. J.,* **57,** 1537–1542.

Flanders, P.J., 1999. Identifying fly ash at a distance from fossil fuel power stations, *Environ. Sci. Technol.,* **33,** 528–532.

Frank, U. & Nowacyk, N.R., 2008. Mineral magnetic properties of artificial samples systematically mixed from haematite and magnetite, *Geophys. J. Int.,* **175,** 449–461.

Guo, H. & Barnard, A.S., 2013. Naturally occurring iron oxide nanoparticles: morphology, surface chemistry and environmental stability, *J. Mater. Chem. A,* 1–27.

Hanesch, M., Stanjek, H. & Petersen, N., 2006. Thermomagnetic measurements of soil iron minerals: the role of organic carbon, *Geophys. J. Int.,* **165,** 53–61.

Hunt, C. P., Moskowitz, B.M. & Banerjee, S.K., 1995. Magnetic properties of rocks and minerals, in *Rock Physics and Phase Relations: A Handbook of Physical Constants,* Vol. 3, pp. 189–204, ed. Ahrens, T.J., American Geophysical Union.

Jordanova, D., Jordanova, N., Atanasova, A., Tsacheva, T. & Petrov, P., 2011. Soil tillage erosion estimated by using magnetism of soils—a case study from Bulgaria, *Environ. Monitor. Assess.,* **183,** 381–394.

Jordanova, D., Jordanova, N. & Werban, U., 2012. Environmental significance of magnetic properties of Gley soils near Rosslau (Germany), *Environ. Earth Sci.*, **69**(5), 1719–1732.

Kapicka, A., Petrovsky, E., Jordanova, N. & Podráizsky, V., 2001. Magnetic parameters of forest topsoils in KrkonoSe Mountains, Czech Republic, *Phys. Chem. Earth* (A), **26**(11–12), 917–922.

King, J., Banerjee, S.K., Marvin, J. & Özdemir, Ö., 1982. A comparison of different magnetic methods for determining the relative grain size of magnetite in natural materials: some results from lake sediments, *Earth planet. Sci. Lett.,* **59,** 404–419.

LeBorgne, E., 1955. Susceptibilité magnétique anormal du sol superficiel, *Annales de Géophysique,* **11,** 399–419.

Lecoanet, H., Leveque, F. & Seguna, S., 1999. Magnetic susceptibility in environmental applications: comparison of field probes, *Phys. Earth planet. Inter.,* **115,** 191–204.

Liu, Q., Hu, P., Torrent, J., Barrón, V., Zhao, X., Jiang, Z. & Sua, Y., 2010. Environmental magnetic study of a Xeralf chronosequence in northwestern Spain: indications for pedogenesis, *Palaeogeog. Palaeclimat. Palaeoecol.,* **293,** 144–156.

Liu, Q., Roberts, A.P., Larrasoaña, J.C., Banerjee, S.K., Guyodo, Y., Tauxe, L. & Oldfield, F., 2012. Environmental magnetism: Principles and applications, *Rev. Geophys.,* **50,** RG4002/2012.

Loosvelt, L., Vernieuwe, H., Pauwels, V.R.N., De Baets, B. & Verhoest, N.E.C., 2013, Local sensitivity analysis for compositional data with application to soil texture in hydrologic modelling. *Hydrol. Earth Syst. Sci.,* **17,** 461–478.

Lu, S.G., Chen, D.J., Wang, S.Y. & Liu, Y.D., 2012. Rock magnetism investigation of highly magnetic soil developed on calcareous rock in Yun-Gui Plateau, China: Evidence for pedogenic magnetic minerals, *J. appl. Geophys.,* **77,** 39–50.

Maher, B.A., 1998. Magnetic properties of modern soils and Quaternary loessic paleosols: paleoclimatic implications, *Palaeogeog. Palaeclimat. Palaeoecol.,* **137,** 25–54.

Maher, B.A., Thompson, R. & Hounslow, M.W., 1999. Introduction, in *Quaternary Climate, Environments and Magnetism,* p. 48, eds Maher, B.A. & Thompson, R., Cambridge Univ. Press.

Mullins, C.E., 1977. Magnetic susceptibility of the soil and its significance in soil science-a review, *Eur. J. Soil Sci.,* **28,** 223–246.

Murray, M.R., 2002. Is laser particle size determination possible for carbonate-rich lake sediments? *J. Paleolimnol.,* **27,** 173–183.

Peters, C. & Dekkers, M., 2003. Selected room temperature magnetic parameters as a function of mineralogy, concentration and grain size, *Phys. Chem. Earth,* **28,** 659–667.

Qin, C-Z., Zhu, A-X., Qiu, W-L., Lu, Y-J., Li, B-L. & Pei, T., 2012. Mapping soil organic matter in small low-relief catchments using fuzzy slope position information, *Geoderma,* **171–172,** 64–74.

Royall, D., 2001. Use of mineral magnetic measurements to investigate soil erosion and sediment delivery in a small agricultural catchment in limestone terrain, *Catena,* **46,** 15–34.

Sadiki, A., Faleh, A., Navas, A. & Bouhlassa, S., 2009, Using magnetic susceptibility to asses soil degradation in the eastern Rif, Morocco, *Earth Surf. Process. Landforms,* **34**(15), 2057–2069.

Schibler, L., Boyko, Ferdyn, T., Gajda, M., Höll, B., Jordanova, S. & Rösler, N.W. Magprox 5 Team., 2002. Topsoil magnetic susceptibility mapping: data reproducibility and compatibility, measurement strategy, *Stud. Geophys. Geod.,* **46,** 43–57.

Singer, M.J., Verousb, K.L., Fine, P. & Tenpas, J., 1996. A conceptual model for the enhancement of magnetic susceptibility in soils, *Quarter. Int.,* **34**–**36,** 243–248.

Suchodoletz, H. von, Kühn, P., Hambach, U., Dietze, M., Zöller, L. & Faust, D., 2009. Loess-like and palaeosol sediments from Lanzarote (Canary Islands/Spain)—indicators of palaeoenvironmental change during the Late Quaternary. *Palaeogeog. Palaeclimat. Palaeoecol.,* **278,** 71–87.

Thompson, R. & Morton, D.J., 1979. Magnetic susceptibility and particle-size distribution in recent sediments of the Loch Lomond drainage basin, Scotland, *J. Sediment. Petrol.,* **49**(3), 801–812.

Thompson, R. & Oldfield, F., 1986. *Environmental Magnetism,* Allen & Unwin, pp. 227.

Torrent, J. & Barrón, V., 2002. Iron oxides in relation to the colour of Mediterranean soils, in *Applied Study of Cultural Heritage and Clays,* Consejo Superior de Investigaciones Científicas, pp. 377–386.

Torrent, J., Liu, Q.S. & Barrón, V., 2010a, Magnetic susceptibility changes in relation to pedogenesis in a Xeralf chronosequence in northwestern Spain, *Eur. J. Soil Sci.,* **61,** 161–173.

Torrent, J., Liu, Q.S. & Barrón, V., 2010b. Magnetic minerals in Calcic Luvisols (Chromic) developed in a warm Mediterranean region of Spain: origin and paleoenvironmental significance, *Geoderma,* **154,** 465–472.

Walden, J., Oldfield, F. & Smith, J.P., 1999. Environmental Magnetism: a practical guide, *Technical Guide,* No. 6, Quaternary Research Association, London.

Williams, R.D. & Cooper, J.R., 1990. Locating soil boundaries using magnetic susceptibility, *Soil Sci.,* **150,** 889–895.

Wilson, J.P. & Gallant, J.C., 2000. *Digital terrain analysis*, in *Terrain Analysis: Principles and Applications*, pp. 27, eds Wilson, J.P. & Gallant, J.C., Wiley.

Worm, H. U., 1998. On the superparamagnetic-stable single domain transition for magnetite, and frequency dependence of susceptibility, *Geophys. J. Int.,* **133,** 201–206.

Zhang, C.X., Quiao, Q., Appel, E. & Huang, B.C., 2012. Discriminating sources of anthropogenic heavy metals in urban street dusts using magnetic and chemical methods, *J. Geochem. Explor.,* **119**–**120**, 60–75.